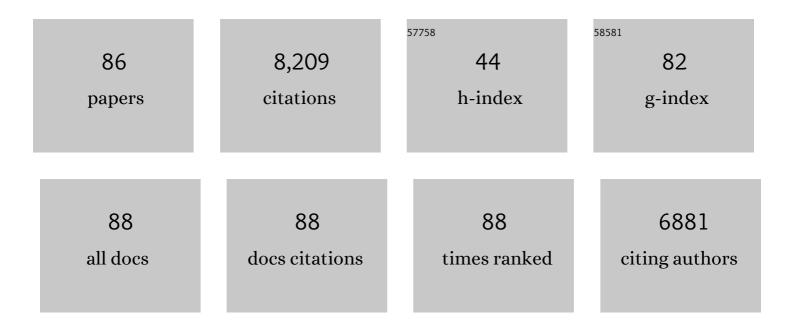
Rahul Banerjee

List of Publications by Year in descending order

Source: https://exaly.com/author-pdf/2412851/publications.pdf Version: 2024-02-01



#	Article	IF	CITATIONS
1	Leveraging hydrogen as the low reactive component in the optimization of the PPCI-RCCI transition regimes in an existing diesel engine under varying injection phasing and reactivity stratification strategies. Energy, 2022, 244, 122629.	8.8	14
2	Dual Nanomechanics in Anisotropic Porous Covalent Organic Framework Janus-Type Thin Films. Journal of the American Chemical Society, 2022, 144, 400-409.	13.7	32
3	A Novel DoE Perspective for Robust Multi-objective Optimization in the Performance-Emission-Stability Response Realms of Methanol Induced RCCI Profiles of an Existing Diesel Engine. Energy, Environment, and Sustainability, 2022, , 347-390.	1.0	2
4	Dual Metalation in a Two-Dimensional Covalent Organic Framework for Photocatalytic C–N Cross-Coupling Reactions. Journal of the American Chemical Society, 2022, 144, 7822-7833.	13.7	102
5	Performance-emission-stability mapping of CI engine in RCCI-PCCI modes under varying ethanol and CNG induced reactivity profiles: A comparative study through experimental and optimization perspectives. Energy, 2022, 254, 124231.	8.8	9
6	Landscaping Covalent Organic Framework Nanomorphologies. Journal of the American Chemical Society, 2022, 144, 11482-11498.	13.7	108
7	Self-Assembly-Driven Nanomechanics in Porous Covalent Organic Framework Thin Films. Journal of the American Chemical Society, 2021, 143, 955-963.	13.7	78
8	Small-Molecule Tunnels in Metalloenzymes Viewed as Extensions of the Active Site. Accounts of Chemical Research, 2021, 54, 2185-2195.	15.6	28
9	Heterogeneous C–H Functionalization in Water via Porous Covalent Organic Framework Nanofilms: A Case of Catalytic Sphere Transmutation. Journal of the American Chemical Society, 2021, 143, 8426-8436.	13.7	65
10	Soluble Methane Monooxygenase Component Interactions Monitored by ¹⁹ F NMR. Biochemistry, 2021, 60, 1995-2010.	2.5	8
11	Parametric sensitivity analysis of split injection coupled varying methanol induced reactivity strategies on the exergy efficiency enhancement and emission reductions objectives in a biodiesel fuelled CI engine. Energy, 2021, 225, 120204.	8.8	20
12	Covalent Organic Frameworks and Supramolecular Nano-Synthesis. ACS Nano, 2021, 15, 12723-12740.	14.6	81
13	Nuclear Resonance Vibrational Spectroscopic Definition of the Fe(IV) ₂ Intermediate Q in Methane Monooxygenase and Its Reactivity. Journal of the American Chemical Society, 2021, 143, 16007-16029.	13.7	24
14	Artificial intelligence assisted MOPSO strategy for discerning the exergy efficiency potential of a methanol induced RCCI endeavour through GA coupled multi-attribute decision making approach. Energy Conversion and Management, 2021, 248, 114727.	9.2	8
15	Nonlinear Rayleigh–Taylor instability with horizontal magnetic field. Indian Journal of Physics, 2020, 94, 927-933.	1.8	5
16	Nanoparticle Sizeâ€Fractionation through Selfâ€Standing Porous Covalent Organic Framework Films. Angewandte Chemie - International Edition, 2020, 59, 1161-1165.	13.8	90
17	Nanoparticle Sizeâ€Fractionation through Self‣tanding Porous Covalent Organic Framework Films. Angewandte Chemie, 2020, 132, 1177-1181.	2.0	27
18	High-Resolution XFEL Structure of the Soluble Methane Monooxygenase Hydroxylase Complex with its Regulatory Component at Ambient Temperature in Two Oxidation States. Journal of the American Chemical Society, 2020, 142, 14249-14266.	13.7	41

#	Article	IF	CITATIONS
19	Structural Studies of the <i>Methylosinus trichosporium</i> OB3b Soluble Methane Monooxygenase Hydroxylase and Regulatory Component Complex Reveal a Transient Substrate Tunnel. Biochemistry, 2020, 59, 2946-2961.	2.5	19
20	Morphological Evolution of Two-Dimensional Porous Hexagonal Trimesic Acid Framework. ACS Applied Materials & Interfaces, 2020, 12, 15588-15594.	8.0	12
21	Connecting Microscopic Structures, Mesoscale Assemblies, and Macroscopic Architectures in 3D-Printed Hierarchical Porous Covalent Organic Framework Foams. Journal of the American Chemical Society, 2020, 142, 8252-8261.	13.7	115
22	Weak Intermolecular Interactions in Covalent Organic Framework-Carbon Nanofiber Based Crystalline yet Flexible Devices. ACS Applied Materials & Interfaces, 2019, 11, 30828-30837.	8.0	54
23	Zinc ion interactions in a two-dimensional covalent organic framework based aqueous zinc ion battery. Chemical Science, 2019, 10, 8889-8894.	7.4	220
24	Porosity Switching in Polymorphic Porous Organic Cages with Exceptional Chemical Stability. Angewandte Chemie, 2019, 131, 4287-4291.	2.0	10
25	Porosity Switching in Polymorphic Porous Organic Cages with Exceptional Chemical Stability. Angewandte Chemie - International Edition, 2019, 58, 4243-4247.	13.8	39
26	Inducing Disorder in Order: Hierarchically Porous Covalent Organic Framework Nanostructures for Rapid Removal of Persistent Organic Pollutants. Journal of the American Chemical Society, 2019, 141, 7572-7581.	13.7	176
27	Triazine Functionalized Porous Covalent Organic Framework for Photo-organocatalytic <i>E</i> – <i>Z</i> Isomerization of Olefins. Journal of the American Chemical Society, 2019, 141, 6152-6156.	13.7	270
28	Covalent Self-Assembly in Two Dimensions: Connecting Covalent Organic Framework Nanospheres into Crystalline and Porous Thin Films. Journal of the American Chemical Society, 2019, 141, 20371-20379.	13.7	166
29	Covalent Organic Frameworks: Chemistry beyond the Structure. Journal of the American Chemical Society, 2019, 141, 1807-1822.	13.7	931
30	Soluble Methane Monooxygenase. Annual Review of Biochemistry, 2019, 88, 409-431.	11.1	124
31	Characterization of performance-emission indices of a diesel engine using ANFIS operating in dual-fuel mode with LPG. Heat and Mass Transfer, 2018, 54, 2725-2742.	2.1	11
32	Ultrastable Imineâ€Based Covalent Organic Frameworks for Sulfuric Acid Recovery: An Effect of Interlayer Hydrogen Bonding. Angewandte Chemie - International Edition, 2018, 57, 5797-5802.	13.8	192
33	Ultrastable Imineâ€Based Covalent Organic Frameworks for Sulfuric Acid Recovery: An Effect of Interlayer Hydrogen Bonding. Angewandte Chemie, 2018, 130, 5899-5904.	2.0	39
34	Supramolecular Reassembly of Selfâ€Exfoliated Ionic Covalent Organic Nanosheets for Labelâ€Free Detection of Doubleâ€Stranded DNA. Angewandte Chemie - International Edition, 2018, 57, 8443-8447.	13.8	140
35	Porosity Prediction through Hydrogen Bonding in Covalent Organic Frameworks. Journal of the American Chemical Society, 2018, 140, 5138-5145.	13.7	118
36	Multi-objective optimization of the performance-emission trade-off characteristics of a CRDI coupled CNG diesel dual-fuel operation: A GEP meta-model assisted MOGA endeavour. Fuel, 2018, 211, 891-897.	6.4	15

#	Article	IF	CITATIONS
37	High-Resolution Extended X-ray Absorption Fine Structure Analysis Provides Evidence for a Longer FeA·A·A·Fe Distance in the Q Intermediate of Methane Monooxygenase. Journal of the American Chemical Society, 2018, 140, 16807-16820.	13.7	82
38	Superprotonic Conductivity in Flexible Porous Covalent Organic Framework Membranes. Angewandte Chemie, 2018, 130, 11060-11064.	2.0	70
39	Superprotonic Conductivity in Flexible Porous Covalent Organic Framework Membranes. Angewandte Chemie - International Edition, 2018, 57, 10894-10898.	13.8	207
40	Multistimuli-Responsive Interconvertible Low-Molecular Weight Metallohydrogels and the in Situ Entrapment of CdS Quantum Dots Therein. Chemistry of Materials, 2018, 30, 4755-4761.	6.7	32
41	Convergent Covalent Organic Framework Thin Sheets as Flexible Supercapacitor Electrodes. ACS Applied Materials & Interfaces, 2018, 10, 28139-28146.	8.0	134
42	Supramolecular Reassembly of Selfâ€Exfoliated Ionic Covalent Organic Nanosheets for Labelâ€Free Detection of Doubleâ€Stranded DNA. Angewandte Chemie, 2018, 130, 8579-8583.	2.0	29
43	Interlayer Hydrogen-Bonded Covalent Organic Frameworks as High-Performance Supercapacitors. Journal of the American Chemical Society, 2018, 140, 10941-10945.	13.7	339
44	Odd–Even Alternation in Tautomeric Porous Organic Cages with Exceptional Chemical Stability. Angewandte Chemie, 2017, 129, 2155-2158.	2.0	32
45	Odd–Even Alternation in Tautomeric Porous Organic Cages with Exceptional Chemical Stability. Angewandte Chemie - International Edition, 2017, 56, 2123-2126.	13.8	55
46	Molecular Level Control of the Capacitance of Two-Dimensional Covalent Organic Frameworks: Role of Hydrogen Bonding in Energy Storage Materials. Chemistry of Materials, 2017, 29, 2074-2080.	6.7	277
47	Constructing Ultraporous Covalent Organic Frameworks in Seconds via an Organic Terracotta Process. Journal of the American Chemical Society, 2017, 139, 1856-1862.	13.7	432
48	Targeted Drug Delivery in Covalent Organic Nanosheets (CONs) via Sequential Postsynthetic Modification. Journal of the American Chemical Society, 2017, 139, 4513-4520.	13.7	475
49	Interplaying anions in a supramolecular metallohydrogel to form metal organic frameworks. Chemical Communications, 2017, 53, 3705-3708.	4.1	20
50	Predesigned Metal-Anchored Building Block for In Situ Generation of Pd Nanoparticles in Porous Covalent Organic Framework: Application in Heterogeneous Tandem Catalysis. ACS Applied Materials & Interfaces, 2017, 9, 13785-13792.	8.0	162
51	Selfâ€Exfoliated Metalâ€Organic Nanosheets through Hydrolytic Unfolding of Metalâ€Organic Polyhedra. Chemistry - A European Journal, 2017, 23, 7361-7366.	3.3	45
52	A porous porphyrin organic polymer (PPOP) for visible light triggered hydrogen production. Chemical Communications, 2017, 53, 4461-4464.	4.1	74
53	Potential for cometabolic biodegradation of 1,4-dioxane in aquifers with methane or ethane as primary substrates. Biodegradation, 2017, 28, 453-468.	3.0	37
54	Selective Molecular Separation by Interfacially Crystallized Covalent Organic Framework Thin Films. Journal of the American Chemical Society, 2017, 139, 13083-13091.	13.7	695

#	Article	IF	CITATIONS
55	Equilibrating (L)Fe ^{III} –OOAc and (L)Fe ^V (O) Species in Hydrocarbon Oxidations by Bio-Inspired Nonheme Iron Catalysts Using H ₂ O ₂ and AcOH. Journal of the American Chemical Society, 2017, 139, 17313-17326.	13.7	48
56	High-Energy-Resolution Fluorescence-Detected X-ray Absorption of the Q Intermediate of Soluble Methane Monooxygenase. Journal of the American Chemical Society, 2017, 139, 18024-18033.	13.7	98
57	Use of Isotopes and Isotope Effects for Investigations of Diiron Oxygenase Mechanisms. Methods in Enzymology, 2017, 596, 239-290.	1.0	13
58	Application of artificial intelligence (AI) in characterization of the performance–emission profile of a single cylinder CI engine operating with hydrogen in dual fuel mode: An ANN approach with fuzzy-logic based topology optimization. International Journal of Hydrogen Energy, 2016, 41, 14330-14350.	7.1	48
59	Performance –emission optimization of a diesel-hydrogen dual fuel operation: A NSGA II coupled TOPSIS MADM approach. Energy, 2016, 117, 281-290.	8.8	47
60	An experimental investigation on the potential of hydrogen–biohol synergy in the performance-emission trade-off paradigm of a diesel engine. International Journal of Hydrogen Energy, 2016, 41, 3712-3739.	7.1	18
61	An experimental based ANN approach in mapping performance-emission characteristics of a diesel engine operating in dual-fuel mode with LPG. Journal of Natural Gas Science and Engineering, 2016, 28, 15-30.	4.4	56
62	Experimental study on the role of ethanol on performance emission trade-off and tribological characteristics of a CI engine. Renewable Energy, 2016, 86, 972-984.	8.9	22
63	An experimental study on combustion, performance and emission analysis of a single cylinder, 4-stroke DI-diesel engine using hydrogen in dual fuel mode of operation. International Journal of Hydrogen Energy, 2015, 40, 8586-8598.	7.1	105
64	Structure of the key species in the enzymatic oxidation of methane to methanol. Nature, 2015, 518, 431-434.	27.8	241
65	Hydrogen-EGR synergy as a promising pathway to meet the PM–NOx–BSFC trade-off contingencies of the diesel engine: A comprehensive review. International Journal of Hydrogen Energy, 2015, 40, 12824-12847.	7.1	64
66	Adaptive-neuro fuzzy inference system (ANFIS) based prediction of performance and emission parameters of a CRDI assisted diesel engine under CNG dual-fuel operation. Journal of Natural Gas Science and Engineering, 2015, 27, 274-283.	4.4	23
67	Development and validation of a GEP model to predict the performance and exhaust emission parameters of a CRDI assisted single cylinder diesel engine coupled with EGR. Applied Energy, 2015, 140, 52-64.	10.1	46
68	ANN metamodel assisted Particle Swarm Optimization of the performance-emission trade-off characteristics of a single cylinder CRDI engine under CNG dual-fuel operation. Journal of Natural Gas Science and Engineering, 2014, 21, 1156-1162.	4.4	26
69	A comparative study of GEP and an ANN strategy to model engine performance and emission characteristics of a CRDI assisted single cylinder diesel engine under CNG dual-fuel operation. Journal of Natural Gas Science and Engineering, 2014, 21, 814-828.	4.4	38
70	Performance and exhaust emissions prediction of a CRDI assisted single cylinder diesel engine coupled with EGR using artificial neural network. Applied Energy, 2014, 119, 330-340.	10.1	190
71	A Taguchi-fuzzy based multi-objective optimization study on the soot-NOx-BTHE characteristics of an existing CI engine under dual fuel operation with hydrogen. International Journal of Hydrogen Energy, 2014, 39, 20276-20293.	7.1	28
72	Application of Grey–Taguchi based multi-objective optimization strategy to calibrate the PM–NHC–BSFC trade-off characteristics of aÂCRDI assisted CNG dual-fuel engine. Journal of Natural Gas Science and Engineering, 2014, 21, 524-531.	4.4	56

#	Article	IF	CITATIONS
73	Development of an ANN based system identification tool to estimate the performance-emission characteristics of a CRDI assisted CNG dual fuel diesel engine. Journal of Natural Gas Science and Engineering, 2014, 21, 147-158.	4.4	74
74	A TMI based CNG dual-fuel approach to address the soot–NOx–BSFC trade-off characteristics of a CRDI assisted diesel engine – an EPA perspective. Journal of Natural Gas Science and Engineering, 2014, 20, 221-240.	4.4	22
75	Multi objective optimization of performance parameters of a single cylinder diesel engine with hydrogen as a dual fuel using pareto-based genetic algorithm. International Journal of Hydrogen Energy, 2014, 39, 8063-8077.	7.1	36
76	An experimental investigation of performance-emission trade off of a CI engine fueled by diesel–compressed natural gas (CNG) combination and diesel–ethanol blends with CNG enrichment. Energy, 2013, 55, 787-802.	8.8	85
77	Multi objective optimization of performance parameters of a single cylinder diesel engine running with hydrogen using a Taguchi-fuzzy based approach. Energy, 2013, 63, 375-386.	8.8	72
78	Intermediate P* from Soluble Methane Monooxygenase Contains a Diferrous Cluster. Biochemistry, 2013, 52, 4331-4342.	2.5	49
79	An experimental study of performance and emission parameters of a compression ignition engine fueled by different blends of Diesel-Ethanol-biodiesel. , 2013, , .		6
80	An Experimental Investigation on the Potential of Hydrogen in the Reduction of the Emission Characteristics of an Existing Four-Stroke Single-Cylinder Diesel Engine Operating Under EGR. International Journal of Green Energy, 2012, 9, 84-110.	3.8	16
81	Effect of viscosity and shear flow on the nonlinear two fluid interfacial structures. Physics of Plasmas, 2012, 19, .	1.9	6
82	An Experimental Investigation on the Role of Hydrogen in the Emission Reduction and Performance Trade-Off Studies in an Existing Diesel Engine Operating in Dual Fuel Mode Under Exhaust Gas Recirculation. Journal of Energy Resources Technology, Transactions of the ASME, 2012, 134, .	2.3	42
83	Combined effect of viscosity and vorticity on single mode Rayleigh–Taylor instability bubble growth. Physics of Plasmas, 2011, 18, .	1.9	25
84	Performance and Emission Characteristic Evaluation of a Single-Cylinder Four-Stroke Diesel Engine Running on Hydrogen and Diesel in Dual Fuel Mode Under Different EGR Conditions. , 2009, , .		3
85	Development of a Neuro Genetic Algorithm Based Virtual Sensing Platform for the Simultaneous Prediction of NOx, Opacity and BSFC in a Diesel Engine Operated in Dual Fuel Mode with Hydrogen under Varying EGR Conditions. SAE International Journal of Engines, 0, 5, 119-140.	0.4	10
86	Characterization of CNG induced transition regimes of reactivity-controlled-combustion of Madhuca longifolia biodiesel: An experimental case study. Energy Sources, Part A: Recovery, Utilization and Environmental Effects, 0, , 1-24.	2.3	6